

NISTIR 6509

**Large Fire Research Facility
(Building 205) Exhaust Hood Heat
Release Rate Measurement System**

David W. Stroup
Laurean DeLauter
Jack Lee
Gary Roadarmel

NIST

National Institute of Standards and Technology
Technology Administration, U.S. Department of Commerce

NISTIR 6509

**Large Fire Research Facility
(Building 205) Exhaust Hood Heat
Release Rate Measurement System**

David W. Stroup
Laurean DeLauter
Jack Lee
Gary Roadarmel
Building and Fire Research Laboratory
National Institute of Standards and Technology
Gaithersburg, MD 20899-8641

July 2000



U.S. Department of Commerce
William M. Daley, Secretary

Technology Administration
*Dr. Cheryl L. Shavers, Under Secretary of
Commerce for Technology*

National Institute of Standards and Technology
Raymond G. Kammer, Director

TABLE OF CONTENTS

	<u>Page</u>
LIST OF TABLES	iv
LIST OF FIGURES	iv
ABSTRACT	1
Introduction	2
Experimental Configuration	2
Heat Release Rate Calculation Methodology.	2
Calibration Experiments	5
Results	6
50 kW Hood.	6
500 kW Hood (Furniture Calorimeter)	7
Main Hood.	8
Uncertainty Analysis	9
Summary	10
References	11

List of Tables

		<u>Page</u>
Table 1.	Sample Natural Gas Heat of Combustion Calculation	13
Table 2.	Summary of Uncertainties for Gas Analysis Equipment	14
Table 3.	Uncertainty Components for Heat Release Rate Calculations	14

List of Figures

		<u>Page</u>
Figure 1.	Plan view showing exhaust hood locations in Large Fire Research Facility	15
Figure 2.	Plot of measured (solid line) and theoretical (solid, straight lines) heat release rates versus time for first test of 50 kW hood with fan operating at half speed	16
Figure 3.	Plot of measured (solid line) and theoretical (solid, straight lines) heat release rates versus time for second test of 50 kW hood with fan operating at half speed	16
Figure 4.	Plot of measured (solid line) and theoretical (solid, straight lines) heat release rates versus for third test of 50 kW hood with fan operating at half speed	17
Figure 5.	Plot of measured (solid line) and theoretical (solid, straight lines) heat release rates versus time for first test of 50 kW hood with fan operating at three-quarter speed	17
Figure 6.	Plot of measured (solid line) and theoretical (solid, straight lines) heat release rates versus time for second test of 50 kW hood with fan operating at three-quarter speed	18
Figure 7.	Plot of measured (solid line) and theoretical (solid, straight lines) heat release rates versus time for third test of 50 kW hood with fan operating at three-quarter speed	18
Figure 8.	Plot of measured versus theoretical heat release rates for all tests using the 50 kW hood	19
Figure 9.	Plot of measured (solid line) and theoretical (solid, straight lines) heat release rates versus time for first test of 500 kW hood (furniture calorimeter) with fan operating at three-quarter speed	19
Figure 10.	Plot of measured (solid line) and theoretical (solid, straight lines) heat release rates versus time for second test of 500 kW hood (furniture calorimeter) with fan operating at three-quarter speed	20
Figure 11.	Plot of measured (solid line) and theoretical (solid, straight lines) heat release rates versus time for third test of 500 kW hood (furniture	

List of Figures (continued)

		<u>Page</u>
	calorimeter) with fan operating at three-quarter speed	20
Figure 12.	Plot of measured (solid line) and theoretical (solid, straight lines) heat release rates versus time for first test of 500 kW hood (furniture calorimeter) with fan operating at full speed	21
Figure 13.	Plot of measured (solid line) and theoretical (solid, straight lines) heat Release rates versus time for second test of 500 kW hood (furniture calorimeter) with fan operating at full speed	21
Figure 14.	Plot of measured (solid line) and theoretical (solid, straight lines) heat Release rates versus time for third test of 500 kW hood (furniture calorimeter) with fan operating at full speed	22
Figure 15.	Plot of measured versus theoretical heat release rates for all tests using the 500 kW hood (furniture calorimeter)	22
Figure 16.	Plot of measured (solid line) and theoretical (dotted lines) for transient “fast” and “slow” t-squared tests using the 500 kW hood (furniture calorimeter) with fan operating at full speed	23
Figure 17.	Plot of measured (solid line) and theoretical (solid, straight line) heat Release rates versus time for first test of main hood	24
Figure 18.	Plot of measured (solid line) and theoretical (dotted line) heat release rates versus time for second test of main hood	24
Figure 19.	Plot of measured (solid line) and theoretical (dotted line) heat release rates versus time for third test of main hood	25
Figure 20.	Plot of measured versus theoretical heat release rates for all tests using the main hood	25
Figure 21.	Plot of measured (solid line) and theoretical (dotted line) for a transient “medium” t-squared test using the main hood	26
Figure 22.	Plot of measured (solid line) and theoretical (dotted lines) for transient “fast” and “slow” t-squared tests using the main hood	26

LARGE FIRE RESEARCH FACILITY (BUILDING 205) EXHAUST HOOD HEAT RELEASE RATE MEASUREMENT SYSTEM

**David W. Stroup, Laurean DeLauter,
Jack Lee and Gary Roadarmel**

Abstract

Rate of heat release is a critical parameter for evaluation of the fire properties of a material. The Large Fire Research Facility at the National Institute of Standards and Technology operates three hoods capable of determining heat release rate from oxygen consumption measurements. This report describes the methodology and apparatus used to measure heat release rate. In addition, the results from several calibration tests conducted in each hood are discussed. The heat release rates determined from hood measurements range from 120 % to approximately 60 % of the theoretical values for the natural gas calibration fires.

Key Words: calorimetry; data analysis; fire data; fire measurements; fire tests; heat release rate; large scale fire tests; oxygen consumption

Introduction

Measurement of the rate at which a burning item releases heat is a critical parameter in fire protection engineering. The heat release rate can be used in the characterization of the hazard represented by a given fuel package. When used as input to a computer fire model, the heat release rate can provide information on fire size, fire growth rate, available egress time, and suppression system impact. The Large Fire Research Facility at the National Institute of Standards and Technology (NIST) has three exhaust hoods for use in determining heat release rate. These hoods operate based on the principle of oxygen consumption calorimetry.

Experimental Configuration

The arrangement of the three exhaust hoods in the NIST Large Fire Research Facility is shown in Figure 1. The 50 kW hood is nominally a 1.22 m square sloping upward at approximately a 45 degree angle to a 0.23 m diameter duct. The 500 kW hood (furniture calorimeter) is a square approximately 3 m on a side. It slopes upward at a 45 degree angle to a 0.5 m diameter duct. The main hood is 4 m by 5 m and slopes upward to a 1.2 m square duct.

During a fire test, data from the various sensors are acquired using a computer-based data acquisition system. The fire test data are recorded on magnetic media for further data reduction and interpretation after the test. Data acquisition and reduction in the Large Fire Research Facility are accomplished using in-house developed computer software.

Heat Release Rate Calculation Methodology

Using the principle of oxygen consumption, it is possible to calculate the heat release rate of burning materials when the products of combustion are collected in an exhaust hood. Thornton [1] found, in 1917, that many organic materials produced almost the same amount of heat per unit mass of oxygen consumed. Hinkley et al. [2] suggested using oxygen concentration in exhaust gases to determine the heat release rate of wood cribs in 1968. Parker [3] used this technique to determine the heat release rate of specimens in the ASTM E84 tunnel test. Huggett [4] calculated an average value for the heat release from a fire involving typical organic fuels to be 13.1 MJ per kilogram of oxygen consumed. According to reference 4, heat release rates calculated based on oxygen consumption compare "favorably" with those derived from conventional calorimetric measurements.

The calculation of heat release rate of fires, burning in normal air, using oxygen consumption requires a minimum of two measurements, the flow rate of the products of combustion through the exhaust system and the oxygen concentration in the exhaust products. Parker [5, 6] presents

several sets of equations for calculating heat release rate using oxygen consumption. The appropriateness of each set of equations depends on the combustion products being measured. A paper by Janssens [7] proposes a form of the equations for calculating heat release rate specifically for full-scale fire test applications. These equations use mass flow rates instead of volumetric flow rates. Volumetric flow rates can lead to confusion because of the need to choose an arbitrary reference temperature and pressure.

Typical measurements obtained in the exhaust stream from a fire test include oxygen concentration, carbon dioxide concentration, carbon monoxide concentration, gas temperature, and pressure. A data reduction program, called RAPID [8], implements equations to calculate gas velocity, mass flow rate, and the associated heat release rate.

The gas velocity is determined from the output of a velocity probe and an adjacent thermocouple. Bi-directional probes are used to obtain velocity data in the Large Fire Research Facility hoods. These velocity probes provide a voltage output proportional to the difference between the static and dynamic pressures exerted by the flow. A bi-directional probe yields velocities within 10 % over an angular range of ± 50 degrees of the probe axis in any direction [9]. Two pressure transducers, 0 Pa to 150 Pa and 0 Pa to 500 Pa, were used to monitor pressure. The equation used in RAPID to convert the probe voltage output to gas velocity is:

$$v = 0.0698 \sqrt{C_{pt} R T} \quad (1)$$

where v = gas velocity (m/s)
 C_{pt} = probe conversion (Pa/volt)
 R = probe voltage reading (volt)
 T = gas temperature (K)

For the 50 kW hood and the 500 kW hood (furniture calorimeter), a single velocity probe and associated thermocouple are placed in each duct approximately along the centerline of the duct. The probe and thermocouple are located at a point beyond flow straightening vanes and approximately 8 duct diameters downstream from the duct entry to ensure a reasonably uniform velocity and temperature profile across the duct cross-section. The main hood contains an array of 9 velocity probes and thermocouples. Unlike the circular cross sections of the 50 kW and 500 kW hoods, the cross section of the main hood duct is square, and it is too large to ensure a uniform flow profile. Therefore, the data acquisition program calculates the velocity at each of the 9 points and uses the average to calculate the mass flow rate.

The mass flow rate of gas in the exhaust duct is determined using the calculated velocity and the measured gas temperature. The equation for mass flow rate is:

$$\dot{m}_e = C v A \rho_{amb} \frac{T_{amb}}{T} \quad (2)$$

where m_e	=	gas mass flow rate (kg/s)
C	=	empirical flow coefficient
v	=	calculated gas velocity (m/s)
A	=	cross sectional area of duct perpendicular to the flow (m ²)
ρ_{amb}	=	density of ambient air (kg/m ³)
T_{amb}	=	temperature of ambient air (K)
T	=	gas temperature (K)

The duct for the 50 kW hood is circular with a diameter of 0.23 m and a cross sectional area of 0.041 m². The 500 kW duct is also circular with a diameter of 0.48 m and a cross sectional area of 0.18 m². The flow coefficient used for these two ducts is 0.824. The duct for the main hood (3 MW) is a 1.22 m square with a cross sectional area of 1.49 m². A flow coefficient of 0.9 is used for this hood. Both of these flow coefficient were determined empirically during undocumented tests.

Using the principle of oxygen consumption, the heat release rate can be obtained from the following set of equations [6]:

$$\dot{q} = \left(E\phi - (E_{CO} - E) \frac{1-\phi}{2} \frac{X_{CO}}{X_{O_2}} \right) \frac{\dot{m}_e}{1 + \phi(\alpha - 1)} \frac{M_r(O_2)}{M_r(E)} (1 - X_{H_2O}^0) X_{O_2}^0 \quad (3)$$

$$\phi = \frac{X_{O_2}^0 (1 - X_{CO_2} - X_{CO}) - X_{O_2} (1 - X_{CO_2}^0)}{X_{O_2}^0 (1 - X_{O_2} - X_{CO_2} - X_{CO})} \quad (4)$$

$$X_{H_2O}^0 = \frac{RH_{amb}}{100} \frac{(0.6107 + 0.06052 T_{amb} - 0.0002088 T_{amb}^2 + 0.00007376 T_{amb}^4)}{P_{amb}} \quad (5)$$

where

q	=	heat release rate (kW)
T_{amb}	=	temperature of ambient air (293.13 K)
P_{amb}	=	pressure of ambient air (101.3 kPa)
RH_{amb}	=	relative humidity of ambient air (50 %)
α	=	combustion expansion factor (1.105)
E	=	heat released per unit mass of oxygen consumed (13.1 MJ/kg of O ₂)
E_{CO}	=	heat released per unit mass of oxygen consumed for combustion of CO to CO ₂ (\approx 17.6 MJ/kg of O ₂)
$M_r(E)$	=	relative molecular mass of exhaust gas (\approx 28.97 kg/kmol)
$M_r(O_2)$	=	relative molecular mass of oxygen (\approx 32 kg/kmol)

$X_{O_2}^0$	=	measured mole fraction of O_2 in the incoming air*
$X_{CO_2}^0$	=	measured mole fraction of CO_2 in the incoming air*
X_{CO}^0	=	measured mole fraction of CO in the incoming air*
X_{O_2}	=	measured mole fraction of O_2 in the exhaust gases*
X_{CO_2}	=	measured mole fraction of CO_2 in the exhaust gases*
X_{CO}	=	measured mole fraction of CO in the exhaust gases*

* as measured in the gas analyzer located downstream of the cold traps and desiccant

The mole fractions of oxygen, carbon dioxide, and carbon monoxide in the exhaust stream are measured continuously using a paramagnetic oxygen analyzer, a nondispersive infrared carbon dioxide analyzer, and a nondispersive infrared carbon monoxide analyzer, respectively. The values for incoming air are determined from concentration measurements of the exhaust gases at the start of each fire test.

Gas sampling is accomplished by withdrawing exhaust gas through a sample probe located in each hood duct near the associated velocity probe(s). The gas sample is passed through two filters to remove soot particles and dried by pulling it through two cold traps and two tubes of desiccants. The sampling line has a nominal internal diameter of 9.5 mm. Each moisture trap tube is 270 mm long with a diameter of 30 mm for an approximate volume of 200 cm³. The cold traps are approximately 190 mm long with an internal diameter of 60 mm for an approximate volume of 500 cm³ for each trap. The sampling system volume is minimized to avoid damping out important peak values in the heat release rate measurements. The moisture trap tubes are tightly packed with chemical absorbent, and the volume of each cold trap is reduced by 70 % with the addition of glass beads.

This sampling train does induce some delay in the measurements. The heat release rate calculation is adjusted to account for the “pumping” delay time associated with each gas measurement (oxygen, carbon dioxide, carbon monoxide). The delay times are determined by injecting carbon dioxide into each hood and measuring the time from injection until onset of changes in oxygen and carbon dioxide measurements are observed. No correction is made for the response times (time constants) of the gas analyzers.

Calibration Experiments

A series of calibration experiments were conducted in the Large Fire Research Facility to examine the heat release rate calibration constants, proper functioning of the instrumentation, and system integrity. The calibration experiments consisted of a series of at least three fire tests conducted under each hood using natural gas fired burners. Different burners were used depending on the maximum fire size desired for each test. In each calibration test, the burner was operated at a minimum of three, approximately steady, heat release rates.

The theoretical heat release was calculated from the volume flow data obtained during a calibration test and the heat of combustion of natural gas. Natural gas, while predominately methane, is composed of a number of different gases. The local gas utility provided component analyses of the natural gas on a daily basis. A sample gas analysis is presented in Table 1. Using the appropriate percentage for each component gas and the associated heat of combustion, the total heat of combustion for the natural gas on any day can be calculated. The heat of combustion was calculated on a wet basis, i.e., all of the water in a vapor state. The volume flow rate of gas was determined using a diaphragm test meter. Revolutions of the meter were timed with a stopwatch, and the average of five readings was used to determine the flow. Gas pressure was measured using a pressure gage with a resolution of ± 3.5 kPa.

The ducts from the 50 kW and 500 kW hoods are connected to a variable speed fan. The fan speed can be adjusted continuously. When using the 50 kW hood and the 0.23 m diameter duct, the fan speed is limited to 75 % of its maximum value. Fan speeds higher than this value produce duct pressures greater than the maximum allowable for one of the two pressure transducers. Calibration tests were conducted for the 50 kW and 500 kW hoods at two different fan speeds to examine the impact on the calculated heat release rate.

Results

50 kW Hood

A series of six tests were conducted under the 50 kW hood. Three tests were conducted with the fan operating at 75 % of maximum (motor speed of 1500 rpm), and three were conducted with the fan at 50 % of maximum (motor speed of 1000 rpm). A 0.2 m square burner, filled with sand, was used for calibration of the 50 kW hood. At ignition, the calibration fire was immediately ramped up to a steady state heat release rate of approximately 20 kW. At the end of 5 min, the heat release rate was increased to 40 kW and maintained for 5 min. The heat release rate was then increased and maintained at 85 kW for an additional 5 min. After this 5 min period, the heat release rate was decreased to 40 kW and held for 5 min. Finally, the heat release rate was again decreased to 20 kW for 5 min before being shutoff.

Figures 2 - 7 present heat release rate results calculated from the measurements obtained during the 6 calibration fire tests. The first three graphs are for the 75 % fan speed and the second set of three figures is for the 50 % speed. The system provides results within 15 % for the heat release rates regardless of fan speed.

Figure 8 presents a comparison between the theoretical and measured heat release rates. The theoretical heat release rate is obtained by multiplying the heat of combustion for natural gas by the measured flow rate of the gas. The dotted line in the Figure represents exact agreement. The

maximum difference between the calculated results and the theoretical values is about 15 % with an average value of 4 %.

500 kW Hood (Furniture Calorimeter)

A series of six tests were conducted under the 500 kW (furniture calorimeter) hood. Three tests were conducted with the fan operating at maximum speed, and three were conducted at 75 % of maximum speed. Since the exhaust duct from the 500 kW hood is larger than that from the 50 kW hood, the pressure transducers remain within range regardless of the fan speed. The fan was operated at two speeds considered typical for potential applications of the system. The system should be capable of determining the heat release rate at any fan speed if accurate velocity measurements are obtained.

A 0.3 m square sand burner was used for calibration of the 500 kW hood. At ignition, the calibration fire was immediately ramped up to a steady state heat release rate of approximately 100 kW. At the end of 5 min, the heat release rate was increased to 200 kW and maintained for 5 min. The heat release rate was then increased and maintained at about 450 kW for an additional 5 min. Finally, the heat release rate was again decreased to 200 kW for 5 min before being shutoff.

Figures 9 - 14 present heat release rate results calculated from the measurements obtained during the 6 calibration fire tests. The first three graphs are for the fan operating at maximum speed and the second set of three figures is for the 75 % speed. As expected, the system successfully calculates the heat release rate regardless of fan speed.

Figure 15 presents a comparison between the theoretical and measured heat release rates. The dotted line in the Figure represents exact agreement. The maximum difference between the calculated results and the theoretical values is approximately 40 %. The average difference is about 13 %. The heat release rate in most cases is calculated to be less than the theoretical heat release rate with the disagreement increasing as the heat release rate increases.

A second set of experiments was conducted under the 500 kW hood using a growing fire designed to test the transient response of the measurement system. The fire was produced using a 0.7 m by 1 m rectangular burner, composed of four elements with individual dimensions of 0.35 m by 0.5 m. The burner was 0.31 m (1 ft) high and was connected to six technical grade (minimum 98 % pure) methane cylinders through a manifold and computer controlled valve system. The computer was programmed to monitor the flow of methane gas through four mass flow controllers arranged in parallel.

The system could be programmed to reproduce any fire with a growth rate proportional to time from ignition to the second power, t -squared [10]. The heat release rate curve produced by the burner is one that follows the fire growth rates used in the 1993 edition of National Fire Protection Association (NFPA) 72 National Fire Alarm Code Appendix B [11]. The fast, medium, and slow fires described by this NFPA standard are based on a wide variety of fires that

grow with the square of time and are sometimes referred to as t-squared (t^2) fires. A fast developing fire is one that would take less than 150 s from the time of open burning until the fire reaches a heat release rate of 1055 kW. A medium developing fire is one that would take more than an additional 150 s, but less than 600 s from the time of open burning until the fire reaches a heat release rate of 1055 kW. A slow developing fire is one that would take 600 s or more from the time of open burning until the fire reaches a heat release rate of 1055 kW. A mathematical representation for these curves is as follows:

$$\dot{q} = \alpha t^2 \quad (6)$$

where: \dot{q} = heat release rate (kW)
 α = coefficient (kW/s²)
 t = time (s)

For the purpose of this experimental series, a “fast” fire reached 1055 kW in 150 s, which corresponds to an α equal to 0.0468 kW/s². A “medium” fire reached 1055 kW in 300 s, which corresponds to an α equal to 0.0117 kW/s². A “slow” fire reached 1055 kW in 600 s, which corresponds to an α equal to 0.00293 kW/s².

The "t-squared" burner was used to produce two heat release rate curves during a test under the 500 kW hood. The theoretical fire growth curves (dotted lines) for a fast and a slow fire are overlaid with the data obtained from the test in Figure 16. The measurement system is able to reflect the transient nature of the fire growth curves.

Main Hood

A series of five tests were conducted under the main hood. Three of the tests were conducted with a 0.3 m square sand burner producing steady state heat release rates, and two tests were conducted using the "t-squared" burner.

The 0.3 m square sand burner was used for the steady heat release rate experiments. At ignition, the calibration fire was immediately ramped up to a steady state heat release rate of approximately 425 kW. At the end of 4 min, the heat release rate was increased to 550 kW and maintained for 4 min. After 8 min from ignition, the burner was shut off.

Figures 17 - 19 present heat release rate results calculated from the measurements obtained during the 3 calibration fire tests. Figure 20 presents a comparison between the theoretical and measured heat release rates. The dotted line in the figure represents exact agreement. The maximum difference between the calculated results and the theoretical values is approximately 20 % with an average of 7 %.

The second set of experiments under the main hood used a growing fire designed to test the responsiveness of the measurement system. Two tests were conducted using the "t-squared"

burner. The first test used the burner to produce a medium growth rate fire. Fast and slow fires were produced in the second test.

The calculated heat release rate results (solid lines) for the two tests and the three theoretical heat release rate curves (dotted lines) are overlaid in Figures 21 and 22. The measurement system is able to reflect the transient nature of the fire growth curves.

Uncertainty Analysis

The results presented in this report are subject to a number of uncertainties. Uncertainty can be categorized as either Type A or Type B. Type A uncertainties can be evaluated using standard statistical methods. Type B uncertainties must be evaluated based on scientific judgment using any available relevant information such as previous measurements, similar experience, equipment specifications, calibration data, and handbook values [12]. To assess Type B uncertainty, the upper and lower bounds for each quantity of interest must be estimated such that the probability of the true value being between the bounds is approximately 100 %. The two types of uncertainty are combined into a "combined standard uncertainty" using the *law of propagation of uncertainty* [12]. Finally, the "expanded uncertainty" which corresponds to the 95 % confidence interval (2σ) is determined by multiplying the combined standard uncertainty by a coverage factor, k , of 2.

The estimated accuracy of the heat release data obtained from the exhaust hoods in the Large Fire Research Facility is influenced by a number of factors. Each of these factors has some uncertainty associated with it. Uncertainty exists in both the calculated heat release rate and the known "theoretical" value.

The first source of uncertainty in the calculated heat release rate is the exhaust system. In order to obtain accurate data for determining heat release rate, the exhaust flow must be well mixed and turbulent when it reaches the sampling point. In addition, the velocity profile should be nearly uniform across the duct. The relative locations of the sampling probes (gas concentration, temperature, velocity) can produce uncertainty in the measured quantities. Probe locations can influence each other by altering the flow, and probes can be oriented improperly relative to the flow. Long term experience in the facility suggest these issues result in an expanded uncertainty of ± 5 % for velocity measurements and ± 5 % for temperature and gas concentration measurements.

Another source of uncertainty is the accuracy of the instruments themselves. Several factors such as noise, drift, ambient temperature, gas stream temperature and pressure, and electromagnetic interference can influence the accuracy of the gas analysis instruments. The impact of these factors on the instrument readings, as specified by the respective manufacturers, is summarized in Table 2. Calibration of the instruments can affect the accuracy. Each instrument is calibrated prior to the start of a test using zero and span gases with known

concentrations. The known concentrations have been verified by the gas supplier and are independently reconfirmed periodically. The uncertainty due to incorrect calibration is estimated to be less than 2 %. Velocities obtained using bidirectional probes are estimated to be within 5 % [9].

Other sources of uncertainty include flow coefficients, expansion factors, sample delay times, and dilution of peak values. The currently used flow coefficients and expansion factors are based on some undocumented calibration tests and theoretical analysis. The data reduction software provides some capability to investigate the impact of changes in these values on the calculated heat release rate. Varying the flow coefficient by $\pm 50\%$ has approximately a $\pm 50\%$ effect on the calculated heat release rate. Increasing the expansion factor by 50 % produces approximately a 50 % decrease in heat release rate. Decreasing the expansion factor to a value less than 1 has a negligible impact on the calculated heat release rate. A certain amount of time is required for a gas sample to reach an analyzer and for the analyzer to respond. This time delay must be accounted for to obtain accurate heat release rate measurements. The delay time ranges from 10 s to 20 s. The impact of varying the time adjustments was investigated using the data reduction software. Various changes in time delays had less than a 5 % impact on calculated heat release rate. In many fire tests, the heat release rate will vary rapidly. In order to properly measure rapid changes, the sampling system volume must be minimized to avoid excessive dampening. The transient heat release rate calibration tests indicate that the system can satisfactorily identify fluctuations in heat release rate associated with “fast” t-squared fires ($\alpha = 0.05$ kW/s). More work is needed to investigate these factors in more detail.

Several factors can influence the accuracy of the known theoretical heat release rate. Uncertainty associated with the assumed heat of combustion can impact the theoretical as well as the measured heat release rate. The flow meter measurement accuracy is estimated to be $\pm 10\%$. The impact of variations in combustion efficiency is estimated to be $\pm 5\%$. Finally, pressure variations are expected to yield an uncertainty of $\pm 2\%$. The uncertainties associated with the instruments used to determine heat release accuracy are summarized in Table 3.

While some of these uncertainties can result in significant errors, they can be minimized to acceptable levels through careful calibration. The two most significant sources of error are more difficult to quantify and eliminate. Leaks in the exhaust gas sampling train can result in significantly underestimating the heat release rate. Similarly, loss of exhaust gas from the collection hood can produce errors. The sampling train is examined for leaks before and after each test. Assessing the integrity of the sampling train during a test is more difficult. Various methods are being evaluated for improving the integrity of the sampling train and eliminating potential loss of exhaust gas from the collection hoods.

Summary

A series of calibration experiments were conducted under the exhaust hoods in the Large Fire Research Facility at the National Institute of Standards and Technology. The experiments were conducted to examine the ability of the system to determine heat release rate from oxygen consumption measurements. The tests included both steady state and transient fire growth rates.

The results indicate a wide variation in the level of agreement between measured and theoretical heat release rate. Heat release rates from the fires were determined from oxygen consumption and velocity measurements. The 50 kW hood showed the best level of agreement with a maximum of 13 % difference. The 500 kW hood provided the high level of difference with a maximum of 40 %. The main hood had a maximum difference between measured and theoretical heat release rate of 20 %. In most cases, the measured values obtained using the 500 kW hood were lower than the theoretical heat release rates with the disagreement increasing at the higher heat release rates. The heat release rate values measured in the main hood were generally higher than the calculated values. These values represent the best estimates of rate of heat release measurements in the three calorimetry hoods in the Large Fire Research Facility for a natural gas calibration fire.

A preliminary analysis of the uncertainty associated with the measurement of heat release rate was conducted as part of this work. This analysis identified a number of issues which can influence the accuracy of the heat release rate measurements. A future study will investigate these issues in greater detail.

References

- [1] Thornton, W., "The Relation of Oxygen to the Heat of Combustion of Organic Compounds," *Philosophical Magazine and J. of Science*, **33**, 1917.
- [2] Hinkley, P., H. Wraight, and A. Wadley, "Rates of Heat Output and Heat Transfer in the Fire Propagation Test," Fire Research Note No. 709, Fire Research Station, Borehamwood, England, 1968.
- [3] Parker, W., "An Investigation of the Fire Environment in the ASTM E-84 Tunnel Test," NBS Technical Note 945, National Bureau of Standards, Gaithersburg, MD, 1977.
- [4] Huggett, C., "Estimation of the Rate of Heat Release by Means of Oxygen Consumption," *J. of Fire and Flammability*, **12**, pp. 61-65, 1980.
- [5] Parker, W., "Calculations of the Heat Release Rate by Oxygen Consumption for Various Applications," NBSIR 81-2427, National Bureau of Standards, Gaithersburg, MD, March 1982.

- [6] Parker, W., "Calculations of the Heat Release Rate by Oxygen Consumption for Various Applications," *J. of Fire Sciences*, **2**, September/October 1984, pp. 380-395, 1984.
- [7] Janssens, M.L., "Measuring Rate of Heat Release by Oxygen Consumption," *Fire Technol.*, **27**, pp. 234-249, 1991.
- [8] Peacock, R.D., J.N. Breese, and C.L. Forney, "A Users Guide for RAPID, Version 2.3," NIST Special Publication 798, National Institute of Standards and Technology, Gaithersburg, MD, January 1991.
- [9] Emmons, H.W., "Vent Flows," The SFPE Handbook of Fire Protection Engineering, Second Edition, Society of Fire Protection Engineers, Bethesda, MD, pg. 2-43, 1995.
- [10] Vettori, R.L., "Effect of an Obstructed Ceiling on the Activation Time of a Residential Sprinkler," NISTIR 6253, National Institute of Standards and Technology, Gaithersburg, MD, November 1998.
- [11] NFPA 72, "Appendix B Engineering Guide for Automatic Fire Detector Spacing," *National Fire Alarm Code*, National Fire Protection Association, Quincy, MA, 1996.
- [12] Taylor, B.N. and C.E. Kuyatt, "Guidelines for Evaluating and Expressing the Uncertainty of NIST Measurement Results," NIST Technical Note 1297, 1994 Edition, National Institute of Standards and Technology, Gaithersburg, MD, September 1994.

Table 1. Sample Natural Gas Heat of Combustion Calculation

Energy Content of Natural Gas					
Component	Volume Fraction (%)	Molecular Weight	Molecular Weight Fraction	H_c (kcal/mol)	H_c F_x (kJ/L)
Methane	94.93318	16.041	15.22823	191.759	30.947293
Ethane	2.788895	30.07	0.838621	341.261	1.617960
Propane	0.506528	44.09	0.223328	484.704	0.417377
i-Butane	0.085614	58.12	0.049759	633.744	0.0922376
n-Butane	0.104749	58.12	0.06088	635.384	0.113145
i-Pentane	0.040068	72.15	0.028909	780.12	0.0531377
n-Pentane	0.030024	72.15	0.021663	782.04	0.0399163
C₆ +	0.083655	107.2169	0.089692	1146.538	0.163053
Nitrogen	0.496727	28	0.139084	0	0
CO₂	0.92905	44	0.408782	0	0
Total	99.99849		17.08895		33.7990

Volumetric Rates from Diaphragm Test Meter			
	Time (s)	Volume (L)	Pressure (kPa)
1	18	141.6	92.7
2	18	141.6	92.4
3	17.9	141.6	92.4
4	18	141.6	92.4
Average	18	141.6	92.5

Ambient Pressure = 101.3 kPa

Ambient Temperature = 298.15 K

Pressure Correction = $(P_{dtm} + P_{amb})/P_{amb} = (92.5 + 101.3)/101.3 = 1.91$

Heat Release Rate = Volumetric Flow Rate x Pressure Correction x Heat of Combustion

Heat Release Rate = $(141.6/18) \times 1.91 \times 33.8$

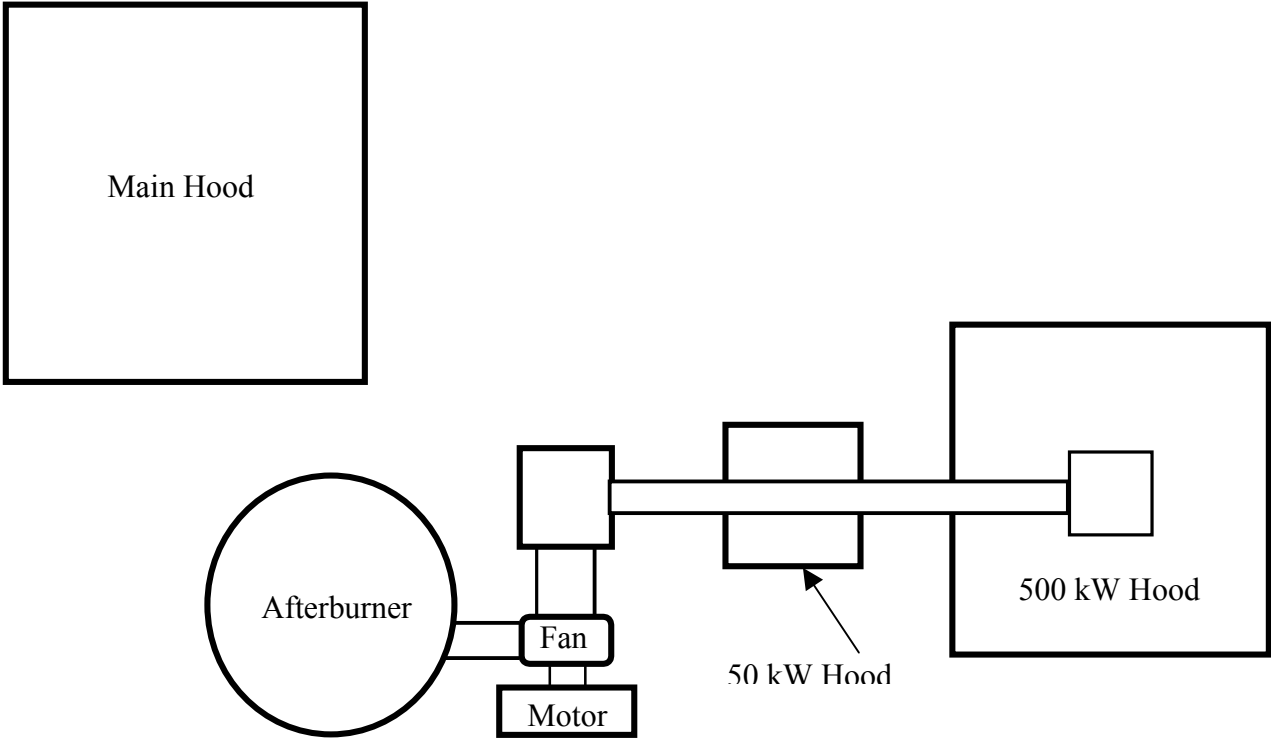
Heat Release Rate = 508 kW

Table 2. Summary of Uncertainties for Gas Analysis Equipment

Factor	Oxygen Meter	CO₂ Meter	CO Meter
Noise		<1 %(smallest span)	<1 %(smallest span)
Zero		<±1 %(span)	<±1 %(span)
Calibration		<±1 %(set point)	<±1 %(set point)
Repeatability	±0.005 %	0.1 % to 1 %(span)	0.1 % to 1 %(span)
Sample Flow	<0.01 %	Negligible	Negligible
Ambient Temp.	<0.02 %	<1 %(span)	<1 %(span)
Flow Pressure		<0.15 %(set point)	<0.15 %(set point)
Power Supply		<0.1 %(signal)	<0.1 %(signal)
RFI Interference	±0.1 %		

Table 3. Uncertainty Components for Heat Release Rate Measurements

Components	Measured	Theoretical
Sample Port		
Velocity	±5 %	
Temp. and Gas Conc.	±1 %	
Bidirectional Probe	±10 %	
Calibration Gas	<2 %	
Coefficients	±15 %	
Delay Times	±5 %	
Heat of Combustion	±5 %	±5 %
Gas Flow Measurement		±10 %
Pressure Measurement		±2 %



Note: Locations are approximate

Figure 1. Plan view showing exhaust hood locations in Large Fire Research Facility

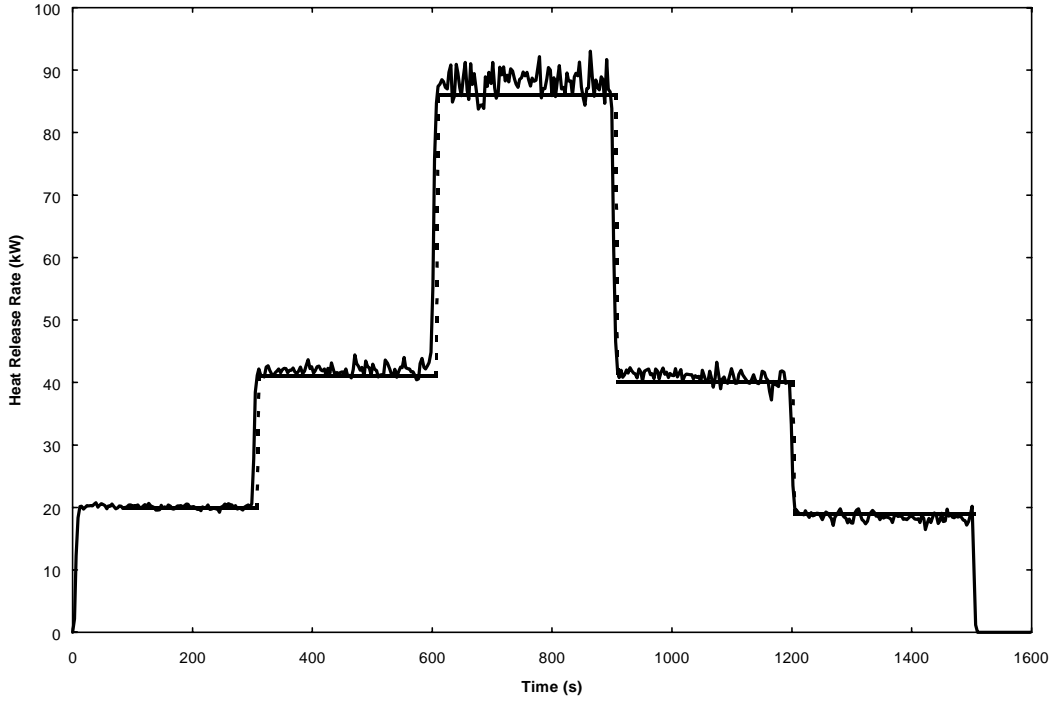


Figure 2. Plot of measured (solid line) and theoretical (solid, straight lines) heat release rates versus time for fire test of 50 kW hood with fan operating at half speed of 50 kW hood with fan operating at half speed

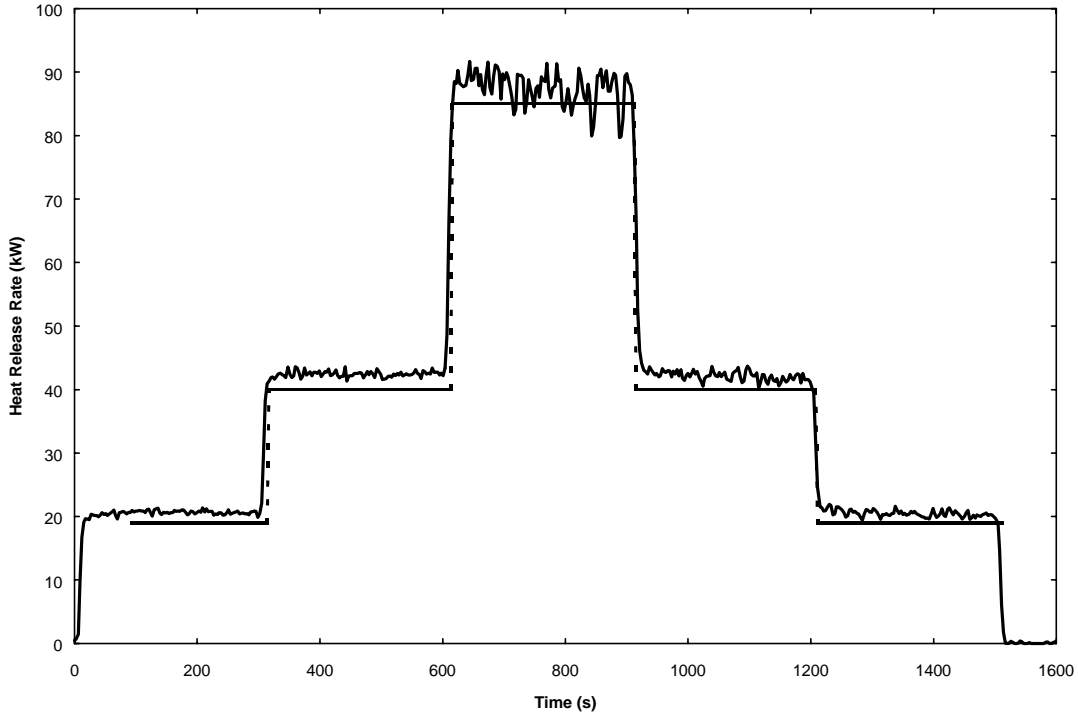


Figure 3. Plot of measured (solid line) and theoretical (solid, straight lines) heat release rates versus time for fire test of 50 kW hood with fan operating at half speed of 50 kW hood with fan operating at half speed

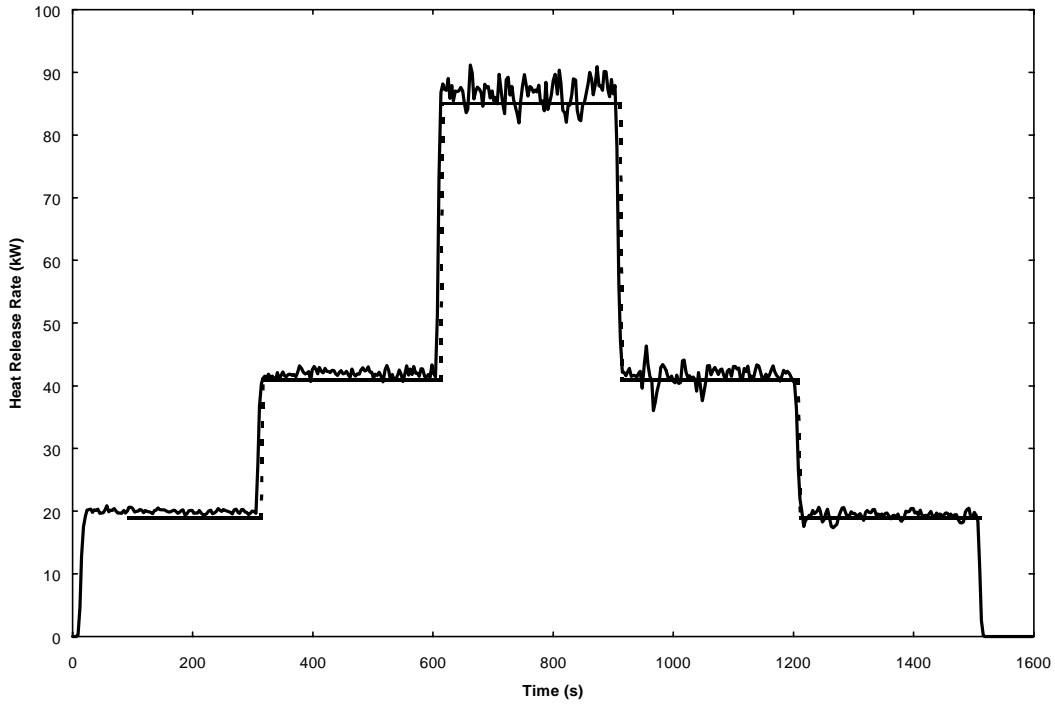


Figure 4. Plot of measured (solid line) and theoretical (solid, straight lines) heat release rates versus for third test of 50 kW hood with fan operating at half speed

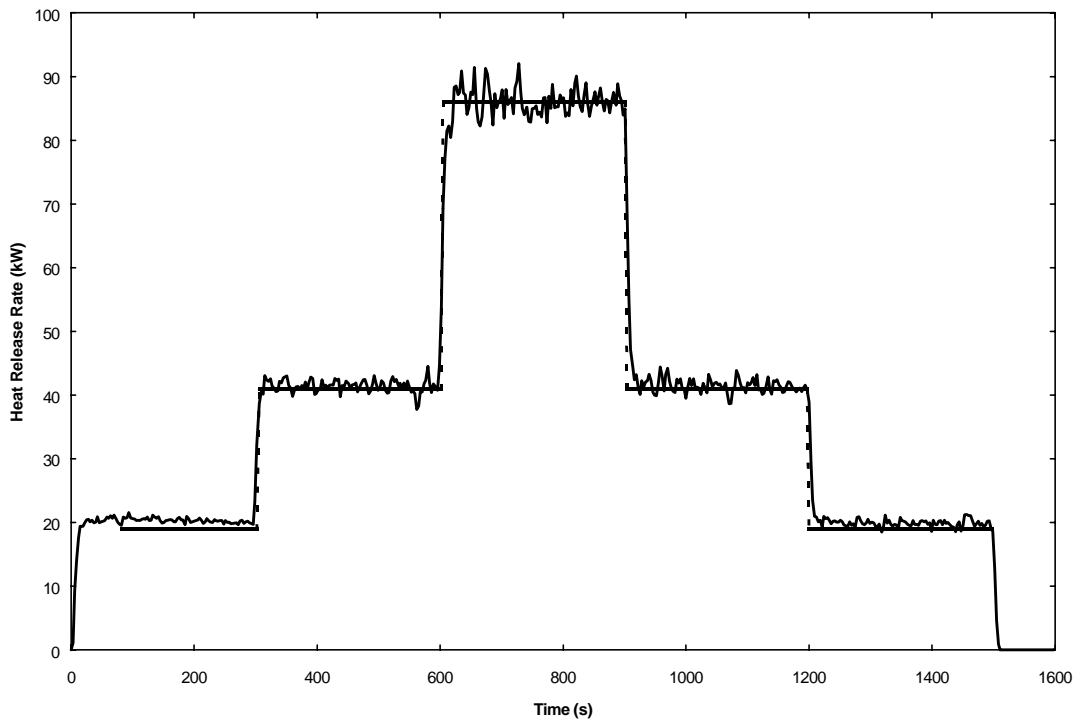


Figure 5. Plot of measured (solid line) and theoretical (solid, straight lines) heat release rates versus time for first test of 50 kW hood with fan operating at three-quarter speed

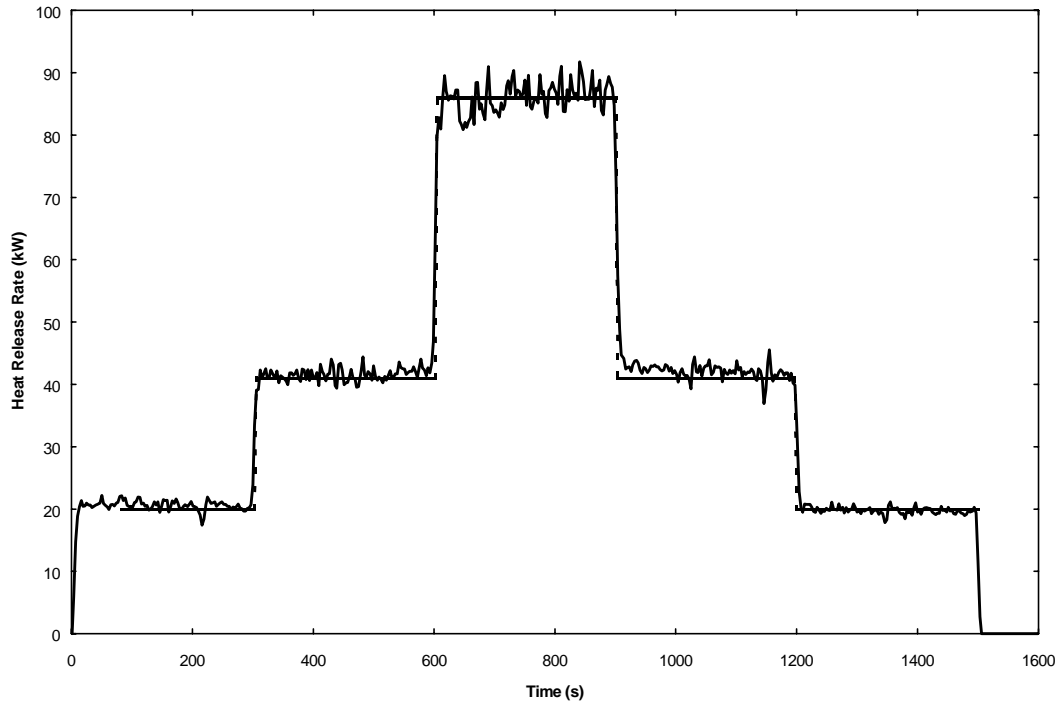


Figure 6. Plot of measured (solid line) and theoretical (solid, straight lines) heat release rates versus time for second test of 50 kW hood with fan operating at three-quarter speed

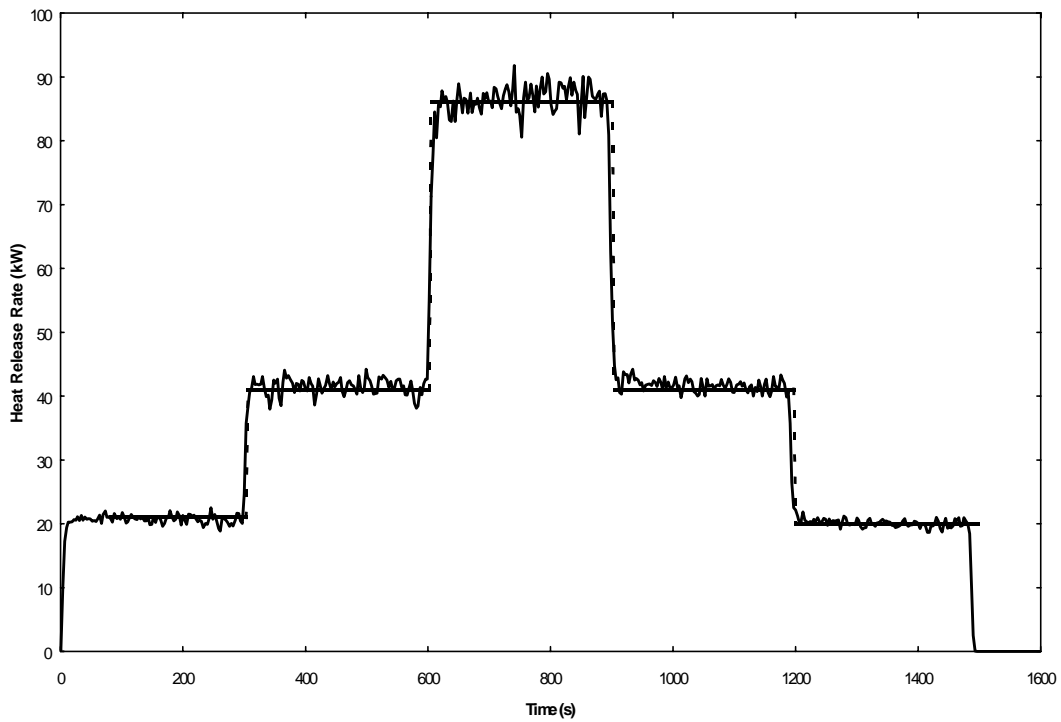


Figure 7. Plot of measured (solid line) and theoretical (solid, straight lines) heat release rates versus time for third test of 50 kW hood with fan operating at three-quarter speed

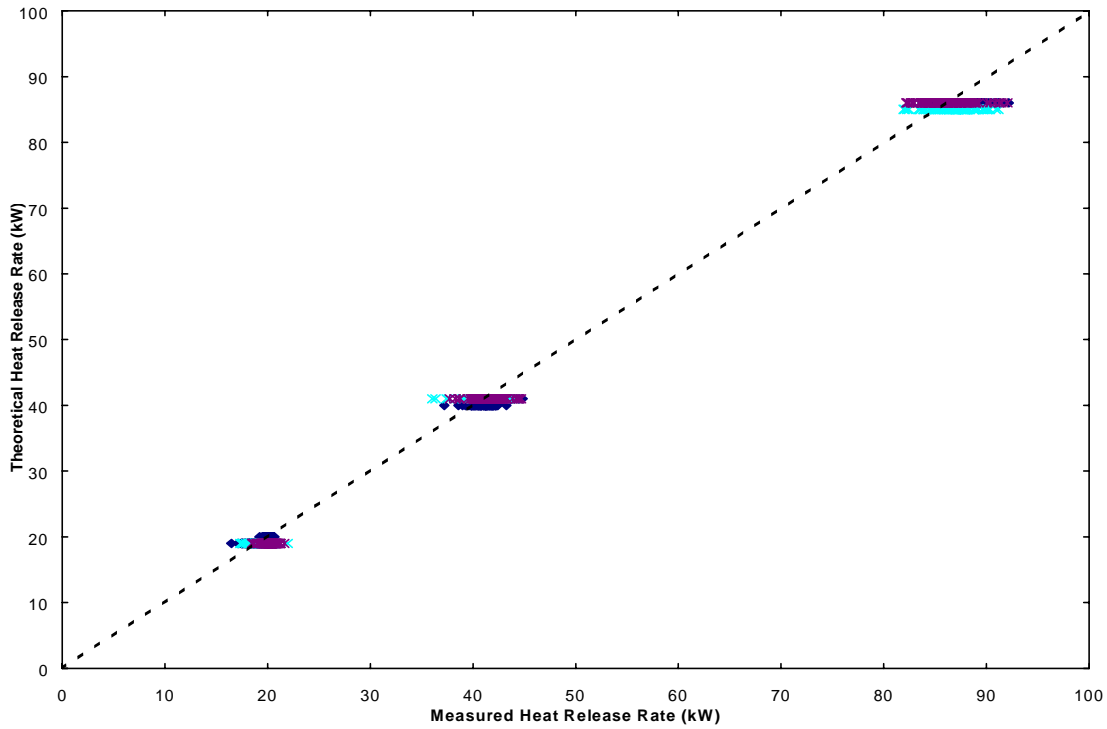


Figure 8. Plot of measured versus theoretical heat release rates for all tests using the 50 kW hood

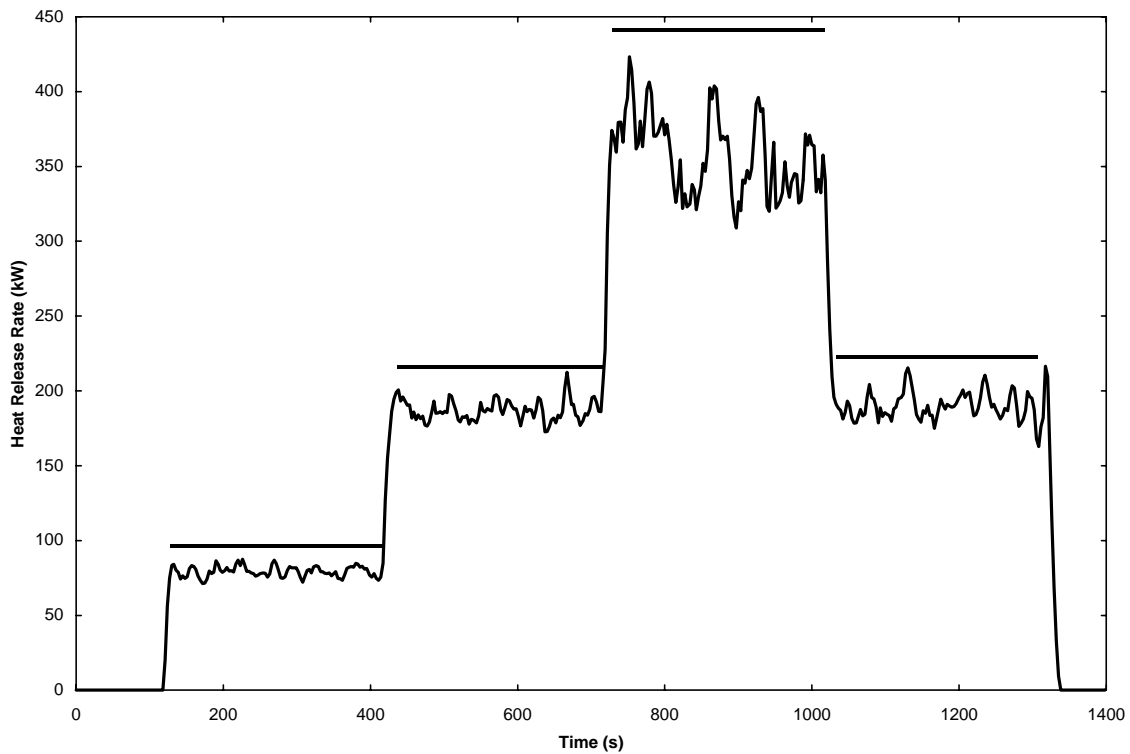


Figure 9. Plot of measured (solid line) and theoretical (solid, straight lines) heat release rates versus time for first test of 500 kW hood (furniture calorimeter) with fan operating at three-quarter speed

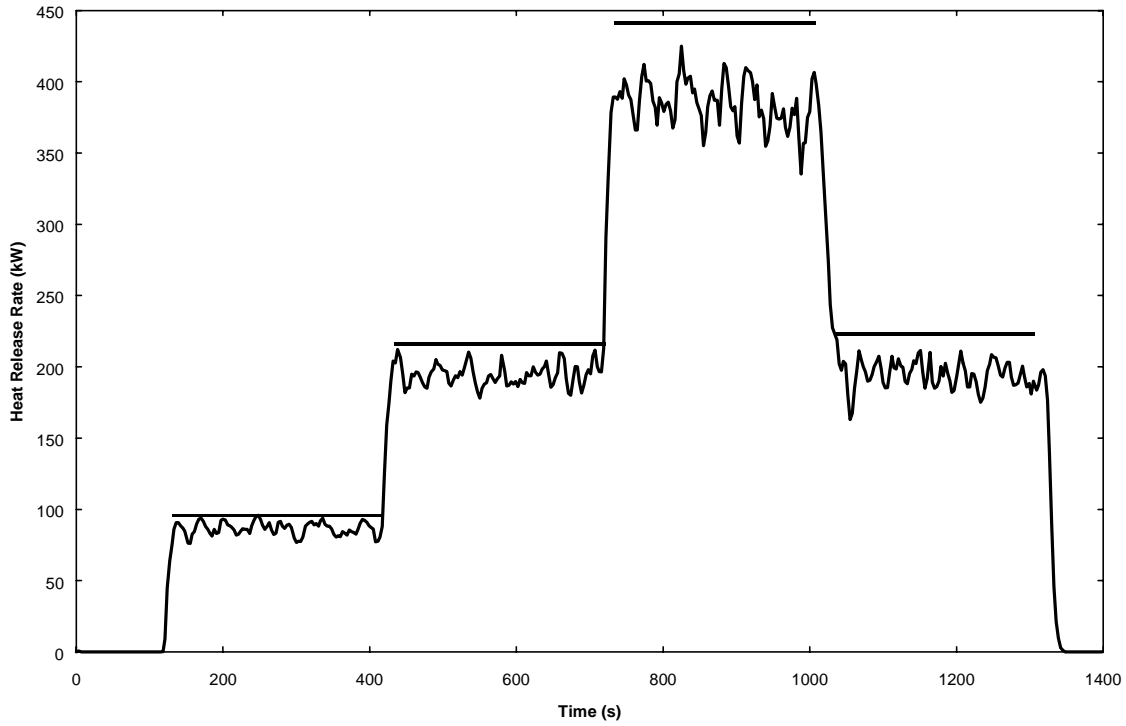


Figure 10. Plot of measured (solid line) and theoretical (solid, straight lines) heat release rates versus time for second test of 500 kW hood (furniture calorimeter) with fan operating at three-quarter speed

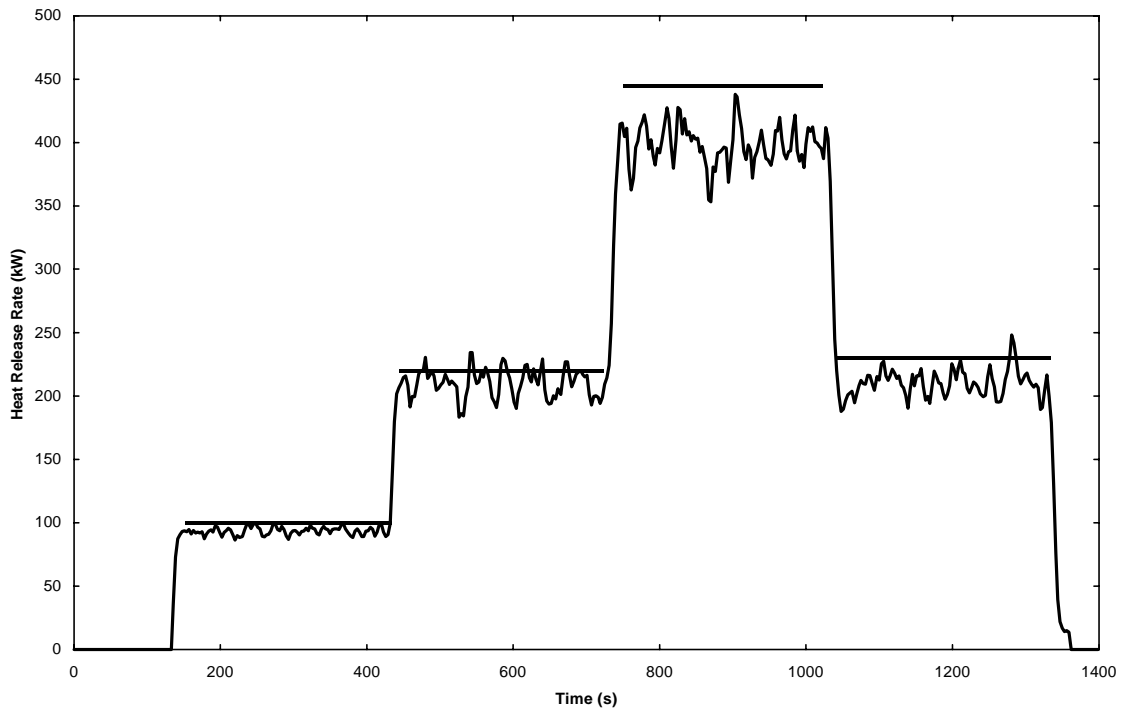


Figure 11. Plot of measured (solid line) and theoretical (solid, straight lines) heat release rates versus time for third test of 500 kW hood (furniture calorimeter) with fan operating at three-quarter speed

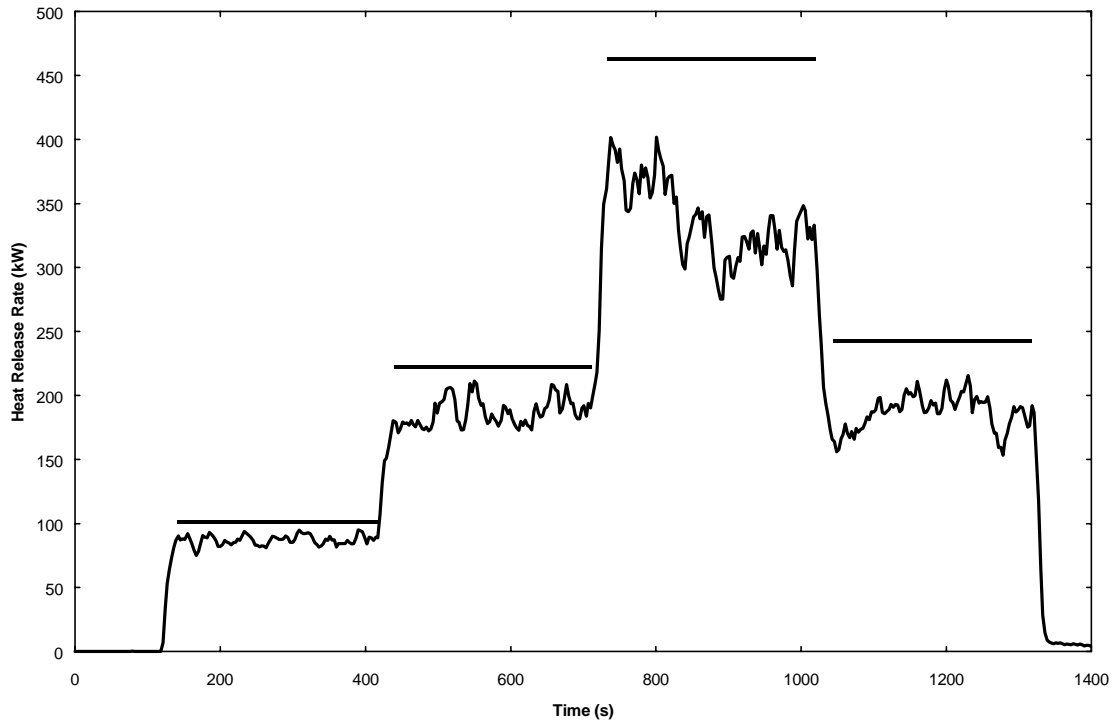


Figure 12. Plot of measured (solid line) and theoretical (solid, straight lines) heat release rates versus time for first test of 500 kW hood (furniture calorimeter) with fan operating at full speed

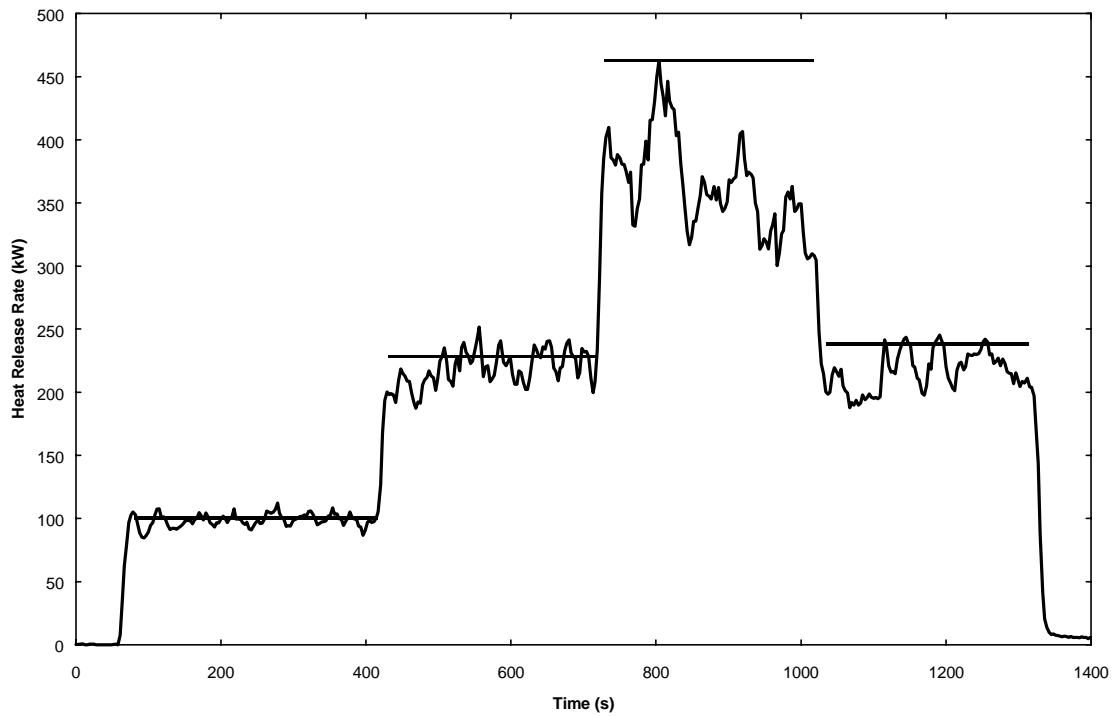


Figure 13. Plot of measured (solid line) and theoretical (solid, straight lines) heat release rates versus time for second test of 500 kW hood (furniture calorimeter) with fan operating at full speed

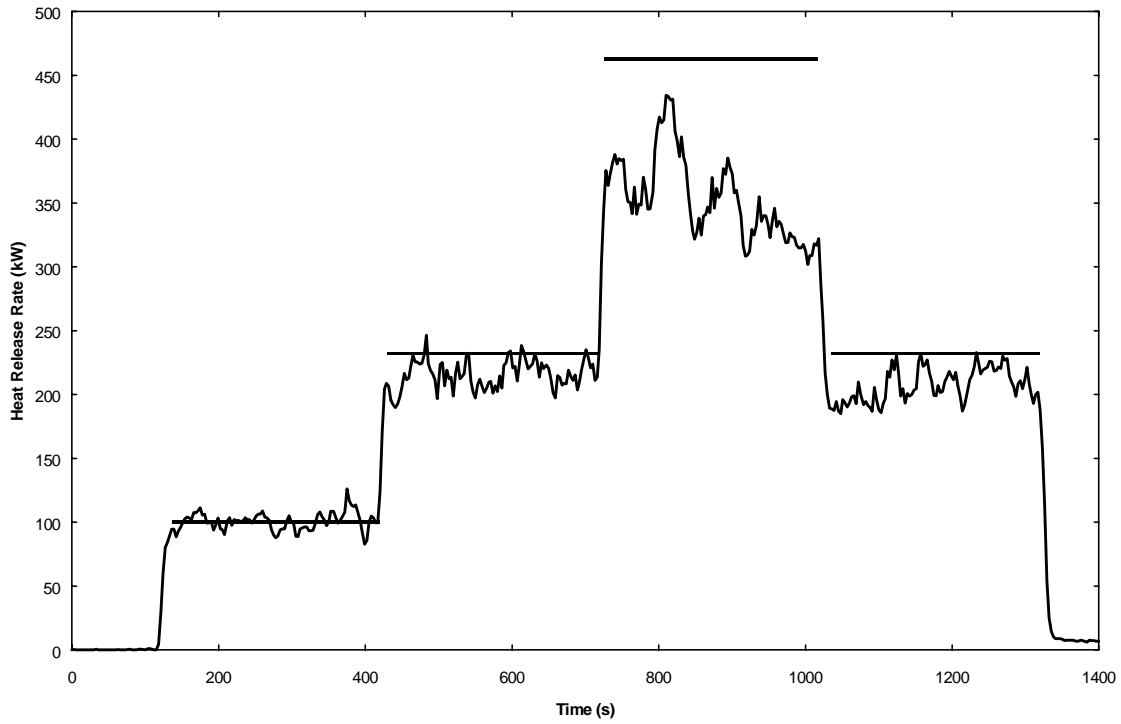


Figure 14. Plot of measured (solid line) and theoretical (solid, straight lines) heat release rates versus time for third test of 500 kW hood (furniture calorimeter) with fan operating at full speed

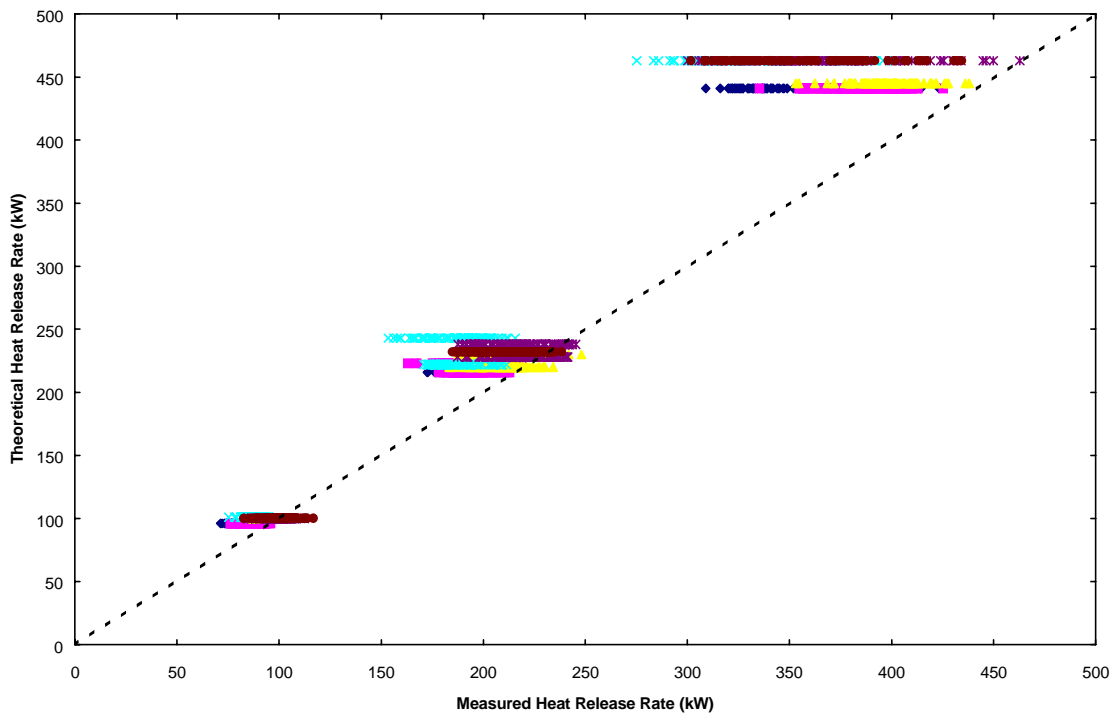


Figure 15. Plot of measured versus theoretical heat release rates for all tests using the 500 kW hood (furniture calorimeter)

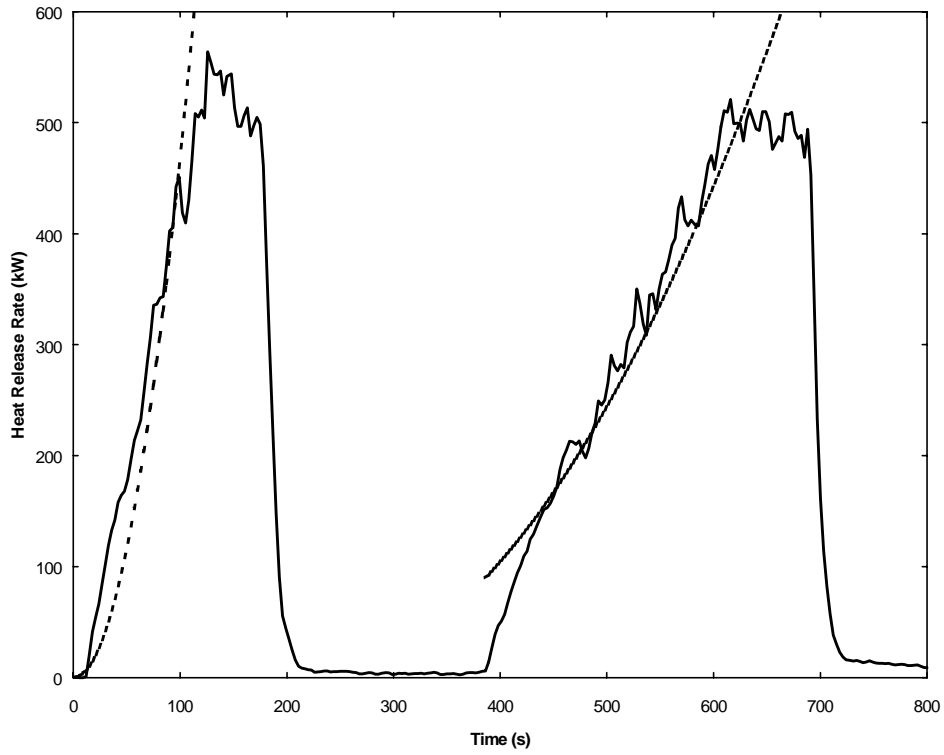


Figure 16. Plot of measured (solid line) and theoretical (dotted lines) for transient “fast” and “slow” t-squared tests using the 500 kW hood (furniture calorimeter) with fan operating at full speed

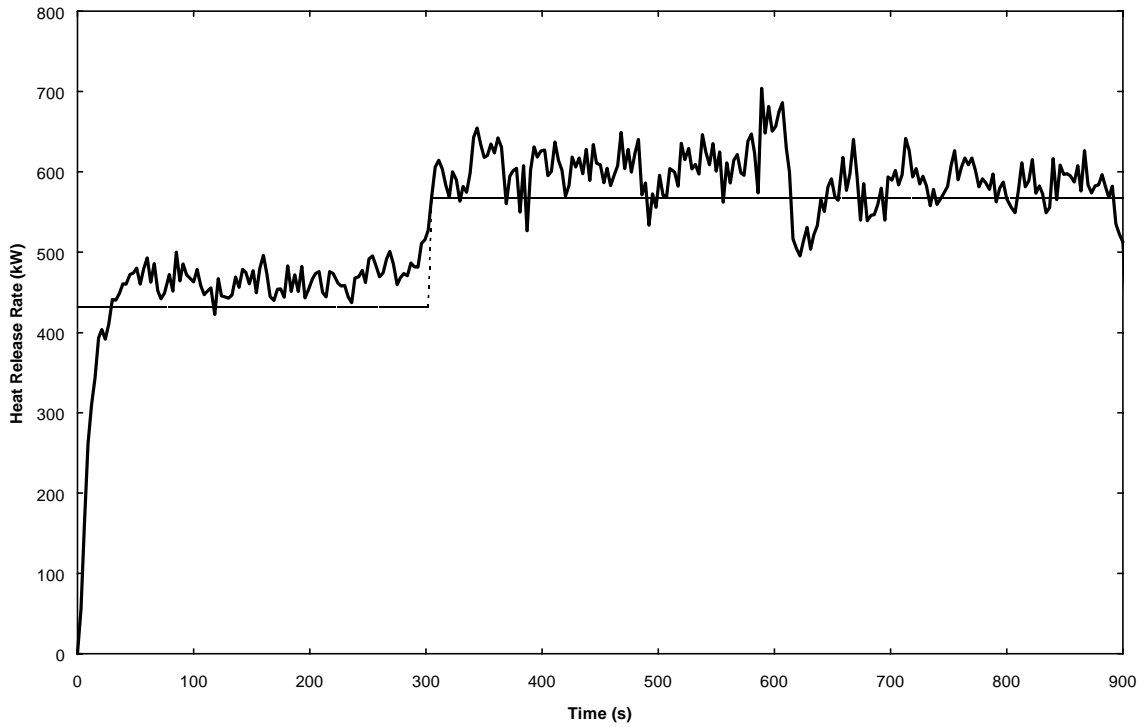


Figure 17. Plot of measured (solid line) and theoretical (solid, straight line) heat release rates versus time for first test of main hood

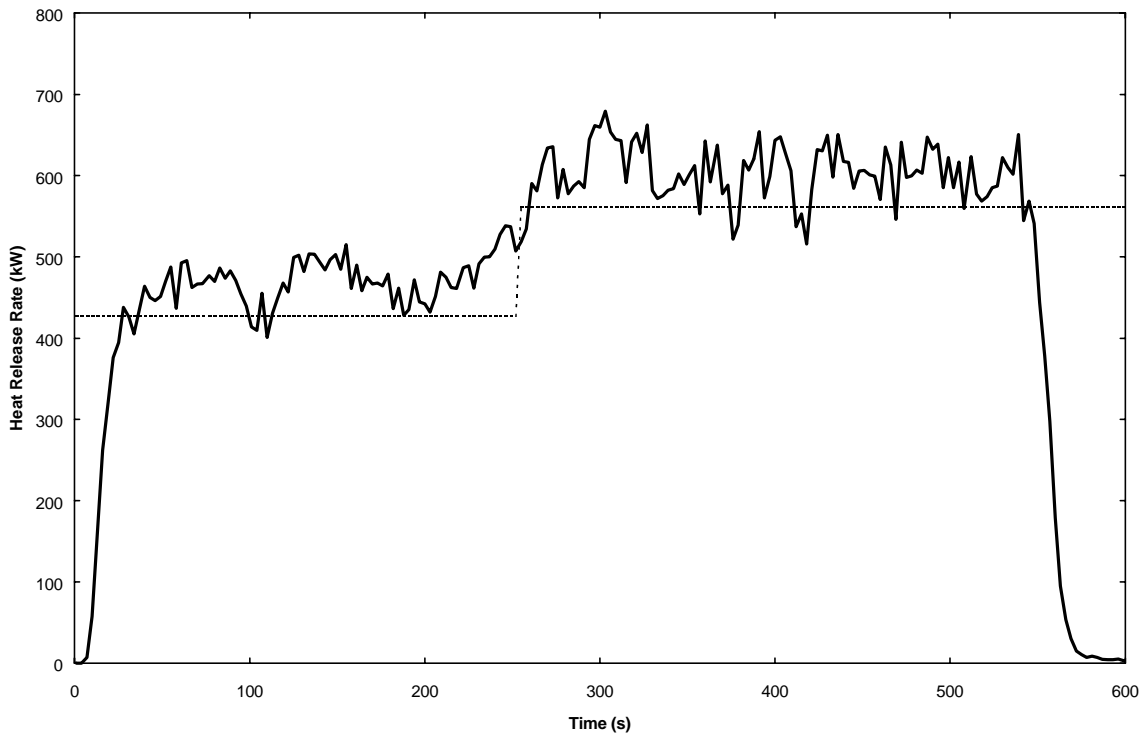


Figure 18. Plot of measured (solid line) and theoretical (dotted line) heat release rates versus time for second test of main hood

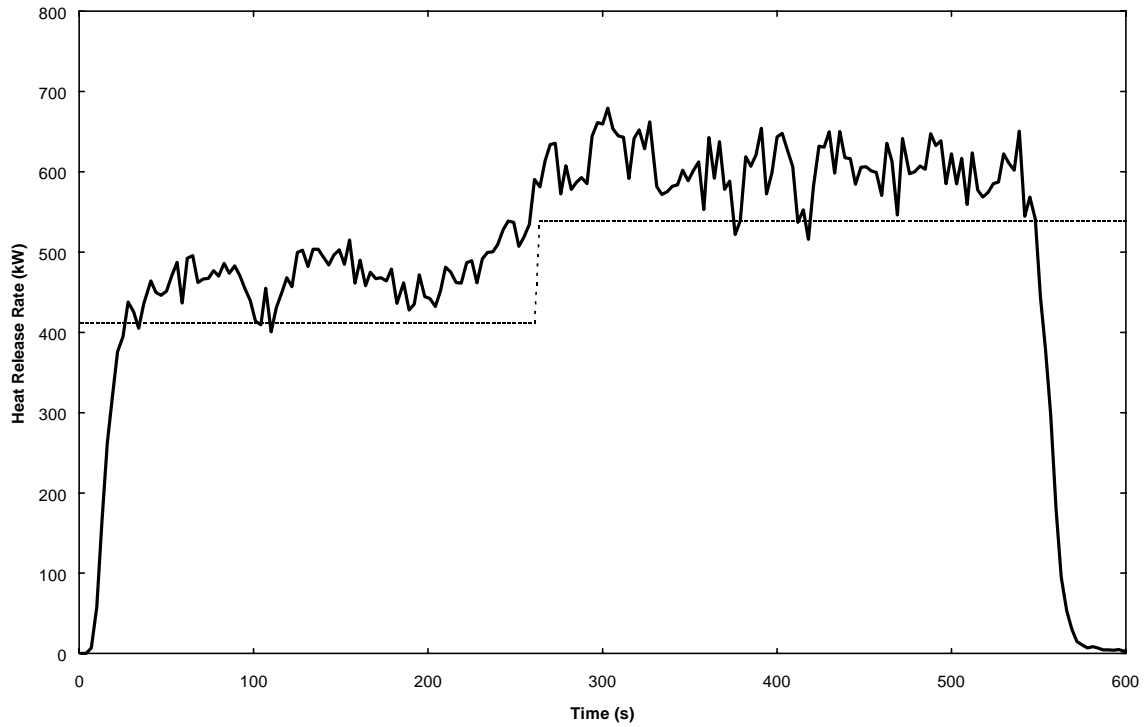


Figure 19. Plot of measured (solid line) and theoretical (dotted line) heat release rates versus time for third test of main hood

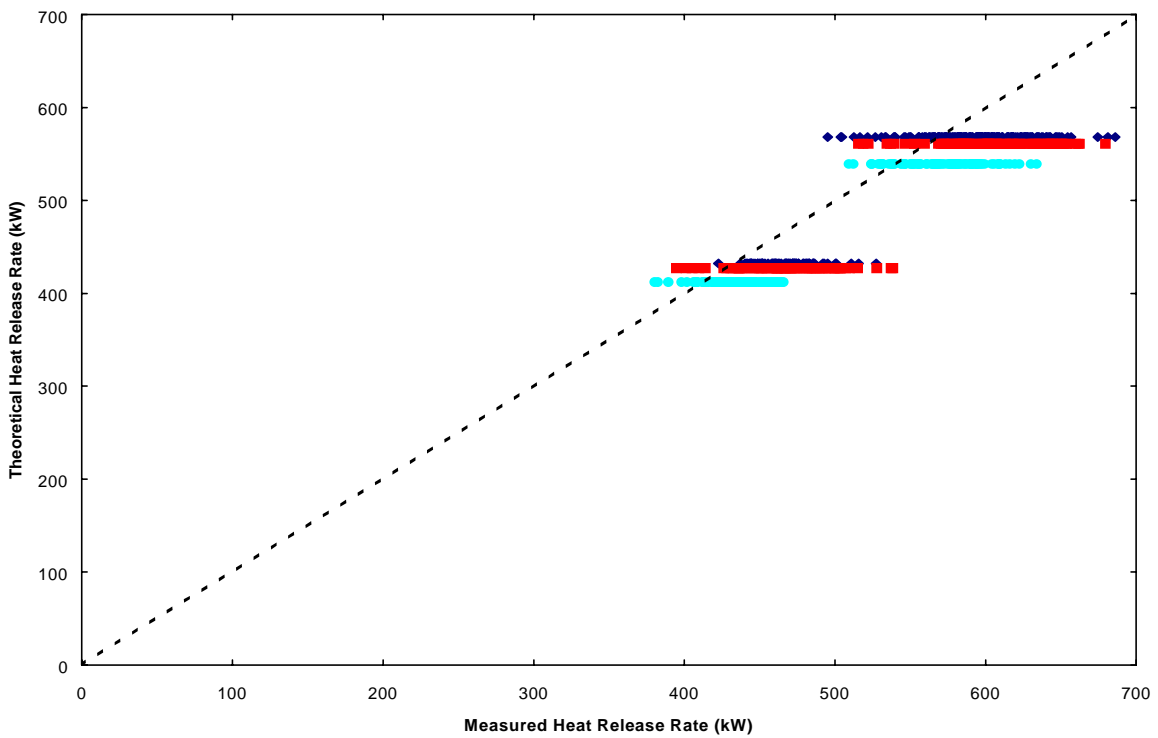


Figure 20. Plot of measured versus theoretical heat release rates for all tests using the main hood

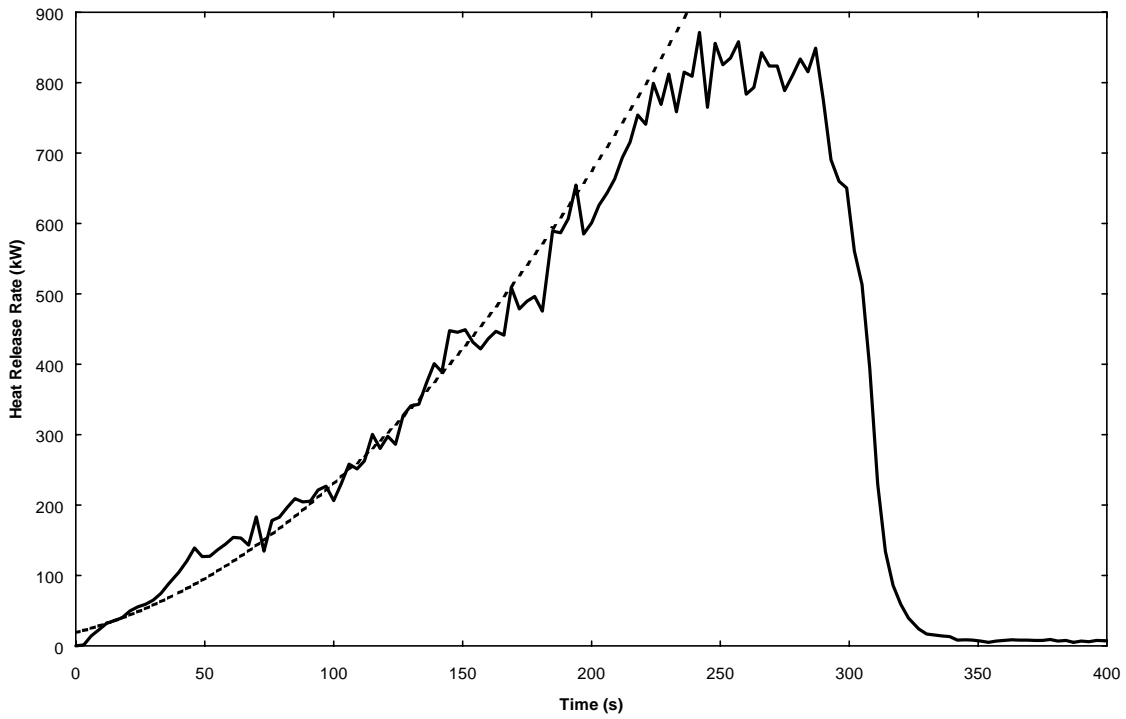


Figure 21. Plot of measured (solid line) and theoretical (dotted line) for a transient “medium” t-squared test using the main hood

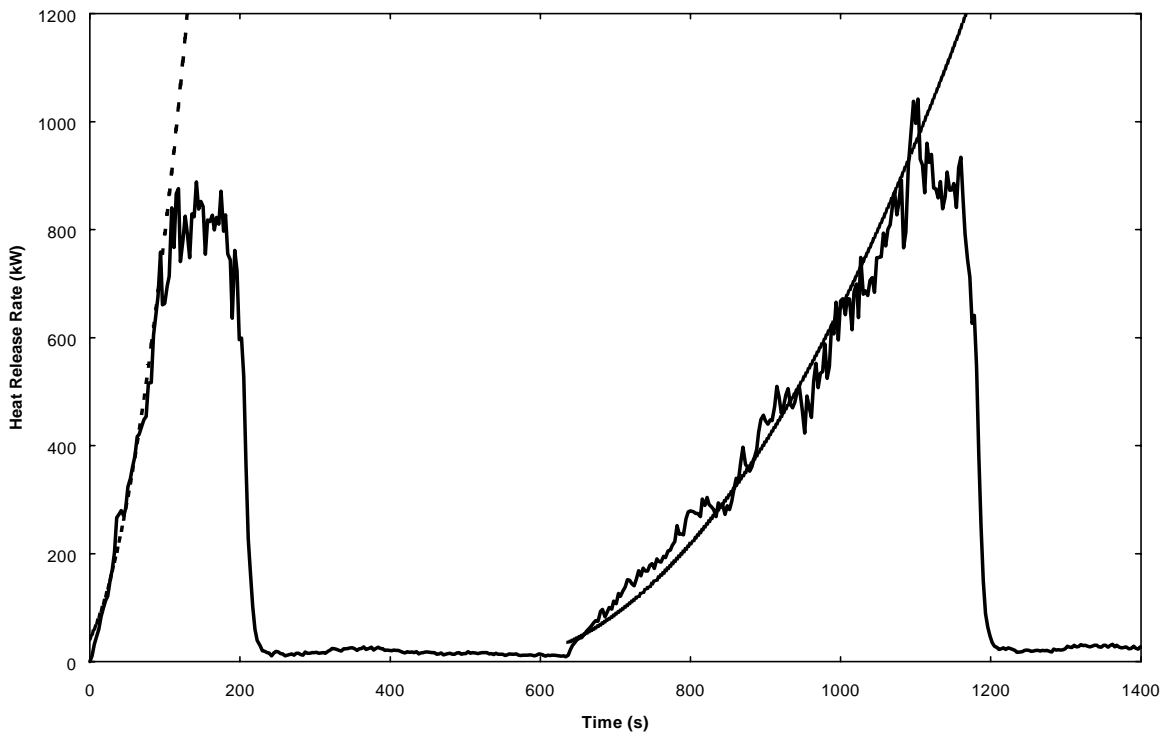


Figure 22. Plot of measured (solid line) and theoretical (dotted lines) for transient “fast” and “slow” t-squared tests using the main hood